ℓ_ε-Regularized Economic Model Predictive Control for Thermal Comfort in Multizone Buildings

Farah Gabsi[1,2], Frederic Hamelin[1], Nathalie Sauer[2] and Joseph J. Yame[1]
[1]*Centre de Recherche en Automatique de Nancy, University of Lorraine, Vandoeuvre-les-Nancy, France*
[2]*Laboratoire de Génie Informatique, de Production et de Maintenance, University of Lorraine, Metz, France*

Keywords: Energy-efficient Buildings, Model Predictive Control, Regularization.

Abstract: This paper presents a new thermal regulation technique for multizone buildings, possibly equipped with discontinuously (on/off) operating HVAC actuators, based on regularized economic model predictive control (REMPC). In the presence of actuators operating on an on/off basis, it often happens that the control scenario resulting from such a strategy is very "aggressive" towards these same actuators due to the many on/off cycles. This phenomenon can lead to premature wear of the actuators most sensitive to these repeated state changes (especially heat pump compressors). In order to take into account the "aggressiveness" of a control scenario and to increase the lifetime of the actuators, an economic criterion with a regularization term based on the parsimony-promoting property of the ℓ_ε-norm (ε small) is used. This term is sufficiently generic to allow the regularization of the optimal control law by taking into account discontinuous control inputs (on/off), reducing the number of actuators used at any given time or avoiding inappropriate control scenarios (alternating use of heat pump in heating/cooling modes,...). To solve the minimization problem of the non-convex ℓ_ε-regularized economic criterion, we use an iterative algorithm recently derived in (Gabsi et al., 2018b). The effectiveness of the proposed control strategy is illustrated on the "Eco-Safe" platform at CRAN Nancy, France.

1 INTRODUCTION

In the context of intelligent buildings, modern centralised automation systems are often used to improve their energy efficiency. "Building Automation and Control Systems" (BACS) are generally based on a dynamic model of buildings. Depending on their complexity and/or performance, they may also include a precise description of the most energy-intensive equipment (heating, ventilation and air conditioning (HVAC) systems (Rawlings et al., 2018),...), the price of electricity or the behaviour of occupants. In addition to this optimized energy management, thermal comfort inside the building is usually a factor taken into consideration, which leads to a global control problem (Gabsi et al., 2018b).

Model Predictive Control (MPC) is one of the most used advanced control strategies in this context, mainly due to its ability to achieve economic objectives, taking into account a simplified dynamic model and different constraints (Godina et al., 2018), (Serale et al., 2018). The modelling method influences the actual practice of MPC in buildings because of its cost and scalability (Gabsi et al., 2017), (Gabsi et al., 2018a), (Zhuang et al., 2018). Economic Model Predictive Control (EMPC) (Zong et al., 2017), (Rawlings et al., 2018), (Ellis et al., 2014) is becoming increasingly popular because of its interest in considering more general economic cost functions than traditional quadratic cost functions.

In recent years, the theory of LASSO (Least Absolute Selection and Shrinkage Operator), particularly used in signal processing, has led to the emergence of new predictive control strategies called "ℓ_{asso} MPC" (Gallieri and Maciejowski, 2012), (Rao, 2018) or RMPC for "Regularized MPC" (Amy et al., 2016). By using penalty criteria in ℓ_1-norm that favor some kinds of sparse controls, it becomes possible, for example, to limit the number of active control inputs in an over-actuated system (Gallieri and Maciejowski, 2015) or to prioritize actuator actions and efficiently distribute control effort (Amy et al., 2016). It is also possible to consider certain control applications that require the use of piecewise constant or impulse-type control signals, with as few changes as possible (Pakazad et al., 2013). In the same way, a binary regularization term can be introduced in order to penalize differently the power variations of actuators depend-

Gabsi, F., Hamelin, F., Sauer, N. and Yame, J.
-Regularized Economic Model Predictive Control for Thermal Comfort in Multizone Buildings.
DOI: 10.5220/0009392801370148
In *Proceedings of the 9th International Conference on Smart Cities and Green ICT Systems (SMARTGREENS 2020)*, pages 137-148
ISBN: 978-989-758-418-3

ing on whether they are in normal operation, startup or shutdown (Cojocaru et al., 2020). Finally, RMPC is also relevant for reducing data packet size in Network Control Systems (NCSs) (Nagahara et al., 2014).

These different problems can also be solved by considering penalties ℓ_0 (Aguilera et al., 2017), (Aguilera et al., 2014), which still have a better parsimonious capacity but make the optimization problem NP-Hard because non-convex. To obtain a continuous but still relatively sparse control, some works use the CLOT (Combined L-One and Two) norm (Challapalli et al., 2017), which is a convex combination of ℓ_1 and ℓ_2-norms and thus allows to benefit from the advantages of each of them.

In this paper, a new predictive control strategy regularized by ℓ_ε-norm penalties is presented. By a judicious choice of the regularization terms, this approach allows in particular to control the solicitations of certain equipments (HVAC,...), for which too frequent starts/stops are critical and are the most energy inefficient method of operating. It also makes it possible to control the number of active control inputs at any time or to avoid inappropriate control scenarios.

The paper is organized as follows. Section 2 first specifies the objectives of the MPC by defining a criterion combining both economic and thermal comfort aspects. The constraints for using different conventional equipments are also specified. Section 3 makes these various objectives explicit in the form of a regularized functional. The proposed strategy is applied to the thermal regulation of buildings in section 4. In particular, CRAN's "Eco-safe" platform is used to highlight the practical value of the proposed approach. Finally, a conclusion and perspectives are presented in Section 5.

2 PROBLEM STATEMENT

This section first defines a criterion for thermal comfort in a multizone building. To satisfy such a criterion while minimizing the energy consumed, a functional is defined as part of the synthesis of a predictive control. Constraints linked to the number of actuators used at any time as well as the variability of the control scenarios are added in order to optimize, among other things, the lifetime of the equipment (heat pump (HP) systems, double flow controlled mechanical ventilation (CMV),...).

2.1 Thermal Comfort

We consider an air volume z_i (hereinafter referred to as zone z_i) delimited by n surfaces (walls, windows, ceiling, floor). Thermal comfort is ensured within this zone if the operative temperature T_{Op,z_i} belongs to a comfort temperature range defined by $T_C \pm 2$ K, where K denotes Kelvin degree.

The operative temperature T_{Op,z_i} can be approached by:

$$T_{Op,z_i} \approx \frac{T_{MR,z_i} + T_{z_i}}{2} \tag{1}$$

where T_{z_i} is the ambient air temperature in zone z_i and T_{MR,z_i} is the mean radiant temperature defined by:

$$T_{MR,z_i} = \frac{\sum_{j=1}^{n} S_{z_i,s_j} \times T_{z_i,s_j}}{\sum_{j=1}^{n} S_{z_i,s_j}} \tag{2}$$

with $\mathbf{T}_{z_i,s} = \left[T_{z_i,s_j}\right]_{1\leq j\leq n}$ representing the temperature of each surface in contact with zone z_i. The contact surface area is assumed to be S_{z_i,s_j}.

As for the comfort temperature, (McCartney and Nicol, 2002) determines it on the basis of studies carried out in situ in buildings. It is a simple linear regression model that fits the filtered temperature T_{RM} of the outside air:

$$T_C = \begin{cases} 0.049\ T_{RM} + 9.2 & \text{if } T_{RM} \leq 283.15 \text{ K} \\ 0.206\ T_{RM} - 34.85 & \text{if } T_{RM} > 283.15 \text{ K} \end{cases} \tag{3}$$

with T_{RM} a temperature that changes daily (D) according to the average outdoor temperature T_{DM} of the previous day ($D-1$):

$$T_{RM}(D) = 0.8T_{RM}(D-1) + 0.2T_{DM}(D-1) \tag{4}$$

2.2 Thermal Model

Before defining the cost function and control constraints, it is necessary to determine a dynamic model reflecting the thermal behaviour of the building by integrating the various equipment as well as all influential disturbances. According to (Gabsi et al., 2018a), the dynamic thermal behavior of a zone z_i delimited by n surfaces (Σ_j) can be represented by the following descriptor time-varying discrete-time system with regular pencil:

$$\begin{cases} \mathbf{E}_{z_i}\mathbf{x}_{z_i}(k+1) = \mathbf{A}_{z_i}\mathbf{x}_{z_i}(k) + \mathbf{F}_{z_i}\mathbf{T}_{\overline{z_i}}(k) + \mathbf{q}_{z_i}(k) + \\ \mathbf{b}_{z_i}^{Sol} q_{z_i}^{Sol}(k)\left(1 - \delta u_{z_i}^{VB}(k)\right) + \mathbf{b}_{z_i}^{TTW}(T_{Ext}(k))u_{z_i}^{TTW}(k) + \\ \mathbf{b}_{z_i}^{HP}(T_{HP},\phi_{HP})u_{z_i}^{HP}(k) + \mathbf{b}_{z_i}^{CMV}(T_{Ext}(k),\mathbf{T}_{\overline{z_i}}(k))u_{z_i}^{CMV}(k) + \\ \quad \ldots \text{(if other equipment is to be considered)} \\ \begin{bmatrix} T_{z_i} \\ \mathbf{T}_{z_i,s} \end{bmatrix}(k) = \mathbf{C}_{z_i}\mathbf{x}_{z_i}(k) \end{cases} \tag{5}$$

with:

- $\mathbf{x}_{z_i}^T(k) = \left[T_{z_i}, \mathbf{T}_{s_i}^T\right](k)$;

- $\mathbf{T}_{s_i}(k)$: the core temperature of each of the surfaces surrounding zone z_i;
- $\mathbf{T}_{\overline{z_i}}(k)$: the ambient air temperature in each of the zones adjacent to zone z_i (possibly including the outside air temperature);
- $\mathbf{q}_{z_i}(k)$: the algebraic value of all incoming and outgoing heat fluxes in z_i; specifically, $q_{z_i}^{Sol}(k)$ reflects incoming short-waves solar radiation.
- $u_{z_i}^{\text{HP}}(k)$, $u_{z_i}^{\text{CMV}}(k)$, $u_{z_i}^{\text{TTW}}(k)$, $u_{z_i}^{\text{VB}}(k),\ldots$: the control inputs in z_i associated with the start-up of HP, CMV, tilt-turn windows (TTW), venetian blinds (VB),...
- $1-\delta u_{z_i}^{\text{VB}}(k)$: the solar heat gain coefficient (SHGC (Cho and Cho, 2018)) with $0 \leq \delta \leq 1$; $u_{z_i}^{\text{VB}}$ depends on whether the blinds are raised ($u_{z_i}^{\text{VB}}=0$) or lowered ($u_{z_i}^{\text{VB}}=1$);
- $T_{Ext}(k)$: the outdoor temperature;
- T_{HP} (vs. ϕ_{HP}): the air temperature (vs. speed) at the heating/cooling system's supply line.

When a building consists of N contiguous zones z_i, the models (5) of each zone can be aggregated, which leads us to consider the time-varying discrete-time system defined as follows:

$$\begin{cases} \mathbf{x}_z(k+1) = \mathbf{A}_z\mathbf{x}_z(k) + \mathbf{F}_T T_{Ext}(k) + \mathbf{F}_q\mathbf{q}_z(k) + \\ \qquad \sum_{\xi=1}^{N_S} \mathbf{B}_\xi\left(\mathbf{x}_z(k), \mathbf{q}_z^{Sol}(k), T_{Ext}(k)\right) u_\xi(k) \\ \begin{bmatrix} \mathbf{T}_z \\ \mathbf{T}_{z,s} \\ \mathbf{T}_{Ext,s} \end{bmatrix}(k) = \mathbf{C}\mathbf{x}_z(k) \end{cases} \tag{6}$$

with:

- $\mathbf{T}_z(k) = \left[T_{z_i}(k)\right]_{1\leq i\leq N}$;
- $\mathbf{T}_{z,s}(k) = \left[\mathbf{T}_{z_i,s}(k)\right]_{1\leq i\leq N}$;
- $\mathbf{u}(k) = \left[u_\xi(k)\right]_{1\leq\xi\leq N_S}$: the control vector defined from the control inputs of all zones z_i. It reflects all possible control scenarios within the multi-zone building (no action, HP (on/off), CMV (on/off), automatic tilt-turn windows (open/close), venetian blinds (open/close),...). Each $u_\xi(k)$ element is equal to either 0 or 1, these two values corresponding respectively to the switching off or switching on of the ξth control input;
- $\mathbf{x}_z^T(k) = \left[\mathbf{T}_z^T, \mathbf{T}_s^T\right](k)$: the state vector defined from vectors $\mathbf{x}_{z_i}(k)$ and $\mathbf{T}_s(k) = \left[\mathbf{T}_{s_i}(k)\right]_{1\leq i\leq N}$;
- $\mathbf{q}_z(k)$: the disturbance vector grouping all heat fluxes into and out of the N zones z_i ; the incoming short-waves solar radiation is specifically reflected by $\mathbf{q}_z^{Sol}(k)$.

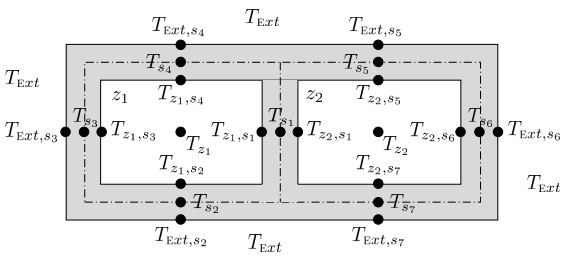

Figure 1: Thermal modeling of a two-zone building.

As an example, the diagram in Fig. 1 represents all the temperatures involved in the thermal modelling of a two-zone building. This simplified sketch, which shows a 2D horizontal cross-sectional view, assumes zones with no ceiling and no floor. 23 temperature nodes are useful for modeling this building: $\mathbf{T}_z \in \mathbb{R}^2$, $\mathbf{T}_{z,s} \in \mathbb{R}^8$, $\mathbf{T}_{Ext,s} \in \mathbb{R}^6$, $\mathbf{T}_s \in \mathbb{R}^7$.

2.3 EMPC - Economic Cost Function and Constraints

The principle of predictive control (Rockett and Hathway, 2017) is to optimize a cost function to describe the control objectives over a forecast time horizon N_P. At each instant k, an optimal control sequence $\{\mathbf{u}^*(k+j))\}_{1\leq j\leq N_P}$ is calculated to minimize this function and only the first element $\mathbf{u}^*(k+1)$ is applied to the system. The economic objective function $J_{\text{MPC}}(\mathbf{u},\mathbf{x})$ that we propose in the context of the thermal regulation of a multizone building is as follows:

$$J_{\text{MPC}}(\mathbf{u},\mathbf{x}) = \min_{\mathbf{u}} \sum_{j=1}^{N_P} \Big(\|\mathbf{T}_{Op}(k+j) - \mathbf{T}_{\text{C}}(k+j)\|_{\Psi_j}^2 + \|\mathbf{u}(k+j)\|_{\epsilon_{\mathbf{u}_j}}^2 + \|\Delta\mathbf{u}(k+j)\|_{\epsilon'_{\Delta\mathbf{u}_j}}^2 \Big) \tag{7}$$

with:

- $\mathbf{T}_{\text{C}}^T(k+j) = \left[T_{\text{C},z_1}(k+j) \ \ldots \ T_{\text{C},z_N}(k+j)\right] \in \mathbb{R}^N$ and $\mathbf{T}_{Op}^T(k+j) = \left[T_{Op,z_1}(k+j)\ldots T_{Op,z_N}(k+j)\right] \in \mathbb{R}^N$ the estimated operative temperature in each zone z_i according to model (6);
- $\|\mathbf{T}_{Op}(k+j) - \mathbf{T}_{\text{C}}(k+j)\|_{\Psi_j}^2 = \sum_{i=1}^{N} \Psi_{z_i,j} \left|T_{Op,z_i}(k+j) - T_{\text{C},z_i}(k+j)\right|^2$
- $\|\mathbf{u}(k+j)\|_{\epsilon_{\mathbf{u}_j}}^2 = \sum_{i=1}^{N}\sum_{\xi=1}^{N_S} \epsilon_{\xi,z_i,j} \left|u_{\xi,z_i}(k+j)\right|^2$;
- $\|\Delta\mathbf{u}(k+j)\|_{\epsilon'_{\Delta\mathbf{u}_j}}^2 = \sum_{i=1}^{N}\sum_{\xi=1}^{N_S} \epsilon'_{\xi,z_i,j} \left|u_{\xi,z_i}(k+j) - u_{\xi,z_i}(k+j-1)\right|^2$

- According to models (5) and (6), all control inputs can be grouped according to the vectors $\mathbf{u}_{z_i}(k)$, $\mathbf{u}(k+j)$ and $\mathbf{u}$ defined as follows:

$$\begin{cases} \mathbf{u}_{z_i}^T(k) = \left[u_{z_i}^{\mathrm{HP}}(k) \;\; u_{z_i}^{\mathrm{CMV}}(k) \;\; u_{z_i}^{\mathrm{TTW}}(k) \;\; u_{z_i}^{\mathrm{VB}}(k)\right] \\ \mathbf{u}^T(k+j) = \left[\mathbf{u}_{z_1}^T(k+j) \;\ldots\; \mathbf{u}_{z_N}^T(k+j)\right] \\ \mathbf{u}^T = \left[\mathbf{u}^T(k+1) \;\ldots\; \mathbf{u}^T(k+N_P)\right] \end{cases} \quad (8)$$

- Weightings $€_{\xi,z_i,j}$ and $€'_{\xi,z_i,j}$ make it possible to specify the cost in euros of each of the possible actions on the system. The €-terms will reflect the energy cost of starting a HP or a VMC for a period of time while the €′-terms will reflect the opening or closing of tilt-turn windows or venetian blinds. As for $\psi_{z_i,j}$, it reflects the importance attached to $T_{\mathrm{O}p,z_i}(k+j)$ being close to $T_{\mathrm{C},z_i}(k+j)$.

Remark 1: The minimization of $J_{\mathrm{MPC}}(\mathbf{u},\mathbf{x})$ (7) requires the calculation of the operative temperature $\mathbf{T}_{\mathrm{O}p}$ in each zone z_i. According to the definition (1), this calculation requires not only the knowledge or estimation of the temperature of each surface in contact with these zones, but also their prediction over the forecast time horizon N_p. In a properly insulated building, since the ambient air temperature in each zone z_i is generally not very different from the mean radiant temperature, it is common to consider $\mathbf{T}_z$ rather than $\mathbf{T}_{\mathrm{O}p}$ in the definition of criterion $J_{\mathrm{MPC}}(\mathbf{u},\mathbf{x})$.

In the long term, the economic cost of a control scenario is not reduced to the mere expression of criterion (7). Indeed, the latter does not take into account abnormal wear and tear or premature failure of actuators, which can generate significant additional costs. In the building context, for example, it is recognized that increasing the number of on/off cycles of a HP compressor increases its electrical consumption but also its wear and tear. Therefore, when synthesizing the control scenario $\{\mathbf{u}^*(k+j)\}_{1\leq j\leq N_P}$ over a horizon N_P, it is important to reduce as much as possible this number of on/off cycles for this equipment.

In order to minimize criterion $J_{\mathrm{MPC}}(\mathbf{u},\mathbf{x})$ while taking into account this last remark, a regularisation term is added.

3 REGULARIZED EMPC (REMPC)

3.1 Regularized Criterion

It is proposed to consider a regularized criterion such as:

$$J_{\lambda,\Omega}(\mathbf{u}) = (1-\lambda)J_{\mathrm{MPC}}(\mathbf{u},\mathbf{x}) + \lambda\Omega(\mathbf{u}) \quad (9)$$

with $J_{\mathrm{MPC}}(\mathbf{u},\mathbf{x})$ defined by (7) and where $0 \leq \lambda \leq 1$ is a regularization parameter. The additional term $\lambda\Omega(\mathbf{u})$ in the criterion amounts to regularizing the solution through a penalty of the latter. In the context of the problem presented before, $\lambda\Omega(\mathbf{u})$ must be a penalty that favours the parsimony of the first derivative of $\mathbf{u}$. Based on Tikhonov's regularization method (Engl et al., 1996), one possible technique is to include a linear operator $\mathbf{R}$ in the regularization term $\Omega(\mathbf{u})$, and solve the following problem :

$$\mathbf{u}^*_{\lambda,p} = \underset{\mathbf{u}\in\mathbb{R}^{n_\mathbf{u}}}{\arg\min}\,(1-\lambda)J_{\mathrm{MPC}}(\mathbf{u},\mathbf{x}) + \lambda\|\mathbf{Ru}\|_p^{\min(1,p)} \quad (10)$$

where $\|\cdot\|_p$ is the ℓ_p-norm $\|\mathbf{w_i}\|_p := \left(\sum_{i=1}^{n_{\mathbf{w_i}}} |w_i|^p\right)^{\frac{1}{p}}$ for a vector $\mathbf{w_i} \in \mathbb{R}^{n_{\mathbf{w_i}}}$. The power $\min(1,p)$ of the regularization term $\|\mathbf{Ru}\|_p^{\min(1,p)}$ makes it possible to consider by continuity the ℓ_∞-norm of $\mathbf{Ru}$ for $p \to \infty$:

$$\lim_{p\to\infty}\|\mathbf{Ru}\|_p^{\min(1,p)} = \lim_{p\to\infty}\left(\sum_i |(\mathbf{Ru})_i|^p\right)^{\frac{1}{p}} = \|\mathbf{Ru}\|_\infty \quad (11)$$

and the ℓ_0-norm of $\mathbf{Ru}$ for $p \to 0$:

$$\lim_{p\to 0}\|\mathbf{Ru}\|_p^{\min(1,p)} = \lim_{p\to 0}\left(\sum_i |(\mathbf{Ru})_i|^p\right) = \|\mathbf{Ru}\|_0 \quad (12)$$

Equation (12) is particularly interesting because, from a theoretical point of view, the parsimony of $\mathbf{Ru}$ is measured using its ℓ_0-norm corresponding to the total number of non-zero elements:

$$\|\mathbf{Ru}\|_0 = \#\left(i \,|\, (\mathbf{Ru})_i \neq 0\right) \quad (13)$$

The linear transform $\mathbf{R}$ can take different forms:

- 0^{th}-order regularization favouring solutions with a small norm:

$$\mathbf{R} = \mathbf{R_0} = \mathbf{I} \quad (14)$$

- 1^{st}-order regularization. It consists in focusing a priori on the low oscillating nature of the solution, and thus penalizing rapid variations:

$$\mathbf{R} = \mathbf{R_1} = \begin{bmatrix} -1 & 1 & 0 & \cdots & \cdots & 0 \\ 0 & \ddots & \ddots & \ddots & & \vdots \\ \vdots & \ddots & \ddots & \ddots & \ddots & \vdots \\ \vdots & & \ddots & \ddots & \ddots & 0 \\ 0 & \cdots & \cdots & 0 & -1 & 1 \end{bmatrix} \quad (15)$$

We notice that at 0^{th}-order, the product $\mathbf{Ru}$ represents a discretization of the vector $\mathbf{u}$, while at 1^{st}-order it is a discretization of its first derivative.

3.2 ℓ_p Penalization

There are several types of penalty functions (Hastie et al., 2009). The Ridge regression corresponds to a penalty of type ℓ_2-norm. As we will see below through a simple example, this function has the particularity of not cancelling the coefficients of **Ru** but rather reducing them and making them tend towards 0. This is a "shrinkage" of coefficients. The Lasso regression, introduced by Tibshirani (Tibshirani, 1994), is a regression penalized by the ℓ_1-norm of the coefficients of **Ru**, which favours parsimony. Fused-Lasso is a variant which allows to take into account the spatiality of the variables (Tibshirani et al., 2005). The objective is to have close estimates for the same variable when they are "close in time". This is made possible by penalizing the ℓ_1-norm of the difference of this variable in two successive instants.

An even more natural penalization than $\|\mathbf{Ru}\|_1$ is to consider a constraint $\|\mathbf{Ru}\|_\varepsilon^\varepsilon$ (with $0 \leq \varepsilon \ll 1$), which not only contracts the value of the different elements of **Ru** but also forces certain elements u_i to be strictly zero for λ large enough thanks to the shape of the isolines of $\|\mathbf{Ru}\|_\varepsilon^\varepsilon$.

By way of illustration, we consider the criterion:

$$J_{\lambda,p}(\mathbf{u}) = (1-\lambda)J^1(\mathbf{u}) + \lambda\|\mathbf{Ru}\|_p^{\min(1,p)} \qquad (16)$$

with $\mathbf{R} = \mathbf{I}$ (14) and $J^1(\mathbf{u}) = (u_1 - 2 + u_2)^2 + (u_2 - 0.5)^2$.

First, we observe that $\forall p \geq 0$, we have:

$$\begin{cases} \mathbf{u}_{0,p}^* = \begin{bmatrix} 1.5 & 0.5 \end{bmatrix}^T = \arg\min_{\mathbf{u}} J^1(\mathbf{u}) \\ \mathbf{u}_{\infty,p}^* = \begin{bmatrix} 0 & 0 \end{bmatrix}^T = \arg\min_{\mathbf{u}} \|\mathbf{Ru}\|_p^{\min(1,p)} \end{cases}$$

Between these two extreme values, the trajectory of $\Gamma_{\lambda,p}$ followed by the minimum $\mathbf{u}_{\lambda,p}^*$ of $J_{\lambda,p}(\mathbf{u})$ as a function of λ is represented in the $u_1 - u_2$ plane in red in Fig. 2. The ellipsoids and the filled contour plot in the background of these figures are isolines of $J^1(\mathbf{u})$ and $\|\mathbf{Ru}\|_p^{\min(1,p)}$ respectively. We can see on each of the subfigures (Fig. 2a-2d) that the shape of the trajectories $\Gamma_{\lambda,p}$ is very different according to the values of p.

In particular, the LASSO selection (Fig. 2c) results in a more parsimonious solution than the Ridge selection (Fig. 2b), which tends to make the coefficients very small without cancelling them. More generally, for $p > 1$, the trajectory $\Gamma_{\lambda,p}$ tends towards $\mathbf{u}_{\infty,p}^*$ for λ increasing but without being "attracted" by the axes $u_1 = 0$ and $u_2 = 0$. On the other hand, as soon as $p \leq 1$, we observe that this convergence towards $\mathbf{u}_{\infty,p}^*$ takes place along one of the axes $u_1 = 0$ or $u_2 = 0$.

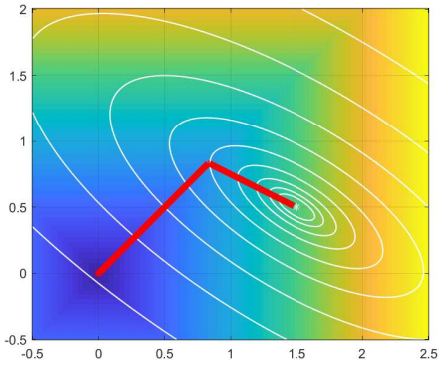

(a) $p \longrightarrow \infty$.

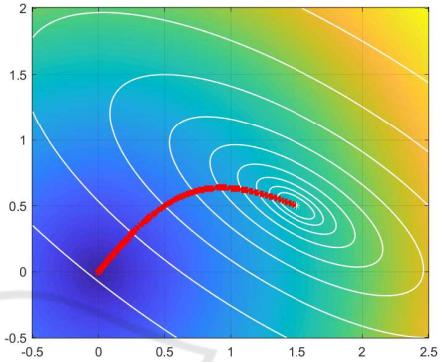

(b) $p = 2$.

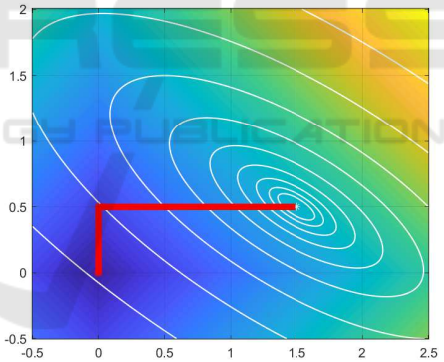

(c) $p = 1$.

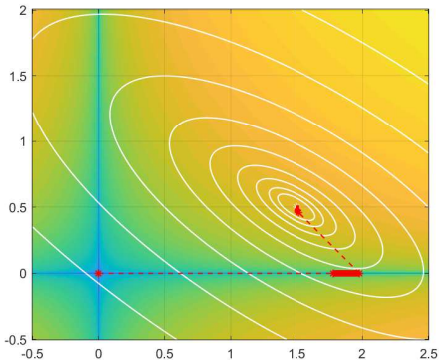

(d) $p = 0.2$.

Figure 2: Trajectory $\Gamma_{\lambda,p}$ (in red) followed by $\mathbf{u}_{\lambda,p}^*$ as a fonction of λ in the $u_1 - u_2$ plane.

In this context ($p \leq 1$), it is interesting to point out the difference in result between a regularization term in ℓ_ε-norm and in ℓ_1-norm. It appears through this example that the axis of attraction can be different ($u_2 = 0$ for ℓ_1-norm (fig. 3c) vs. $u_1 = 0$ for $\ell_{0.2}$-norm (fig. 3d)). Given the shape of the isolines of $J^1(\mathbf{u})$, the preferred solution (in the sense of minimizing the criterion $J^1(\mathbf{u})$) is the one associated with the lowest p-value. Another phenomenon appears for $p < 1$; the trajectory $\Gamma_{\lambda,p}$ followed by $\mathbf{u}^*_{\lambda,p}$ becomes discontinuous as the value of p decreases. This is due to the non-convexity of the term $\|\mathbf{Ru}\|_p^p$ which increases for small values of p and makes the criterion $J_{\lambda,p}(\mathbf{u})$ non-convex.

4 APPLICATION TO THERMAL COMFORT IN MULTIZONE BUILDINGS

4.1 Regularized Criterion

With regards to the regularization term $\Omega(\mathbf{u})$, the following specifications are formulated:

- the number of on/off cycles for HP and CMV in all zones z_i should be limited. In view of the previous paragraph, the minimisation of norms $\sum_{i=1}^{N} \left\|\mathbf{R_1 u}_{z_i}^{\text{HP}}\right\|_\varepsilon^\varepsilon$ and $\sum_{i=1}^{N} \left\|\mathbf{R_1 u}_{z_i}^{\text{CMV}}\right\|_\varepsilon^\varepsilon$ reflects this dual objective with:

$$\begin{cases} \mathbf{u}_{z_i}^{\text{HP}} = \left[u_{z_i}^{\text{HP}}(k) \mid \hat{u}_{z_i}^{\text{HP}}(k+1) \ldots \hat{u}_{z_i}^{\text{HP}}(k+N_P)\right]^T \\ \mathbf{u}_{z_i}^{\text{CMV}} = \left[u_{z_i}^{\text{CMV}}(k) \mid \hat{u}_{z_i}^{\text{CMV}}(k+1) \ldots \hat{u}_{z_i}^{\text{CMV}}(k+N_P)\right]^T \end{cases}$$

- the number of effective actuators should be limited at each time of prediction $k+j$ and in each zone z_i. This specification translates as minimizing the term $\sum_{i=1}^{N} \left\|\mathbf{R_0 u}_{z_i}(k+j)\right\|_\varepsilon^\varepsilon$ with $\mathbf{u}_{z_i}(k+j)$ the control vector defined by (8);
- the control inputs take values in the discrete set $\{0,1\}$ (on/off or open/closed). The minimization of the norm $\|\mathbf{R_0}(\mathbf{u} \odot (\mathbf{u}-\mathbf{1}))\|_\varepsilon^\varepsilon$ meets this objective by defining by $\mathbf{u} \odot (\mathbf{u}-\mathbf{1})$ the element-wise product of two vectors $\mathbf{u}$ and $(\mathbf{u}-\mathbf{1})$.

  For illustration purposes, the trajectory of $\Gamma_{\lambda,p}$ followed by the minimum $\mathbf{u}^*_{\lambda,p}$ of $J_{\lambda,p}(\mathbf{u}) = (1-\lambda)J^1(\mathbf{u}) + \lambda\|(\mathbf{u} \odot (\mathbf{u}-\mathbf{1}))\|_p^{\min(1,p)}$ as a function of λ is represented in the $u_1 - u_2$ plane in red in Fig. 3. For this example, we observe that $\Gamma_{\lambda,p}$ tends towards $\begin{bmatrix}1 & 1\end{bmatrix}^T = \begin{bmatrix}\text{on} & \text{on}\end{bmatrix}^T$, which is the on/off control associated with the lowest value of $J^1(\mathbf{u})$. For this type of regularization, the choice of a ℓ_ε-norm is also justified because the appearance of the isolines $J^1(\mathbf{u})$ is not modified by considering $J_{\lambda,0}(\mathbf{u})$ knowing that $\|\mathbf{u} \odot (\mathbf{u}-\mathbf{1})\|_0 = dim(\mathbf{u}) = 2$ for all $\mathbf{u}$ except for axes $u_1 = 0$ and $u_2 = 0$. This property is interesting because the sole purpose of this regularization term is to impose discrete values on $\mathbf{u}$ and not to modify the shape of the isolines;

  Therefore, $\Omega(\mathbf{u})$ is defined as:

$$\begin{aligned} \Omega(\mathbf{u}) = \alpha_1 &\left\| \mathbf{R_0} \left(\bigodot_{i=1}^{\text{NB}} (\mathbf{u} - u_i \mathbf{1}) \right) \right\|_\varepsilon^\varepsilon \\ &+ \sum_{i=1}^{N} \left(\alpha_2 \left\|\mathbf{R_1 u}_{z_i}^{\text{HP}}\right\|_\varepsilon^\varepsilon + \alpha_3 \left\|\mathbf{R_1 u}_{z_i}^{\text{CMV}}\right\|_\varepsilon^\varepsilon \right) \\ &+ \alpha_4 \sum_{i=1}^{N} \sum_{j=1}^{N_P} \left\|\mathbf{R_0 u}_{z_i}(k+j)\right\|_\varepsilon^\varepsilon \end{aligned} \quad (17)$$

with:

- $\mathbf{u}$ and $\mathbf{u}_{z_i}(k+j)$: augmented control vectors (8);
- $\bigodot_{i=1}^{\text{NB}} (\mathbf{u} - u_i\mathbf{1}) = (\mathbf{u} - u_1\mathbf{1}) \odot \ldots \odot (\mathbf{u} - u_{\text{NB}}\mathbf{1})$ where $\odot$ is the element-wise product of two vectors and $(u_i)_{1 \leq i \leq \text{NB}}$ represent some constant values that can be taken by at least one of the control inputs. For on/off controls, we have $\text{NB} = 2$, $u_1 = 1$ (on) and $u_2 = 0$ (off);
- $\mathbf{u}_{z_i}^{\text{TTW}} = \left[u_{z_i}^{\text{TTW}}(k) \mid \hat{u}_{z_i}^{\text{TTW}}(k+1) \ldots \hat{u}_{z_i}^{\text{TTW}}(k+N_P)\right]^T$;
- $\mathbf{u}_{z_i}^{\text{VB}} = \left[u_{z_i}^{\text{VB}}(k) \mid \hat{u}_{z_i}^{\text{VB}}(k+1) \ldots \hat{u}_{z_i}^{\text{VB}}(k+N_P)\right]^T$.

An α_2 (or α_3) that tends towards 0 will generally cause permanent stress on the associated actuator, which will affect its lifetime. Conversely, an α_2 (or α_3) that tends towards infinity ensures a low stress on the actuator but thermal comfort performance can them become poor according to criterion $J_{\text{MPC}}(\mathbf{u},\mathbf{x})$ because the solution obtained then becomes too far from the optimal non-regularized solution.

4.2 Minimisation of the Regularized Criterion

The closed-loop REMPC requires an optimal solution to (9) at each step. It is usually very difficult to quickly find optimal solutions (and prove their optimality) for non-convex problems. First of all, it is important to mention that the minimization of the

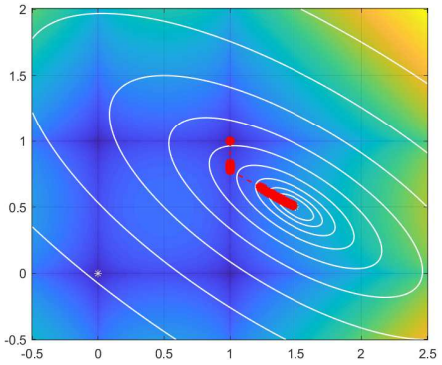

(a) $p = 0.6$.

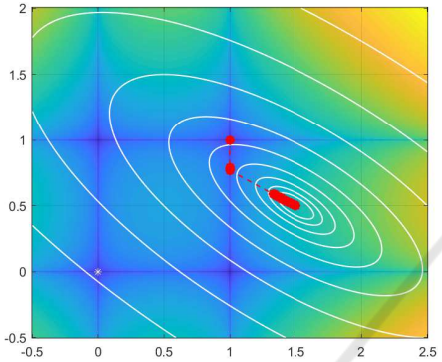

(b) $p = 0.4$.

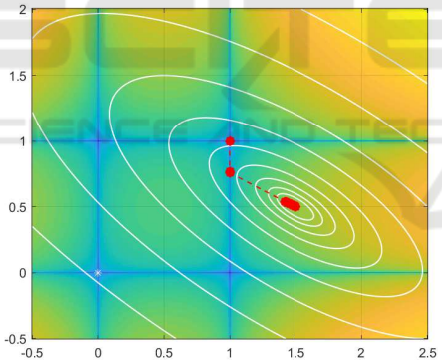

(c) $p = 0.2$.

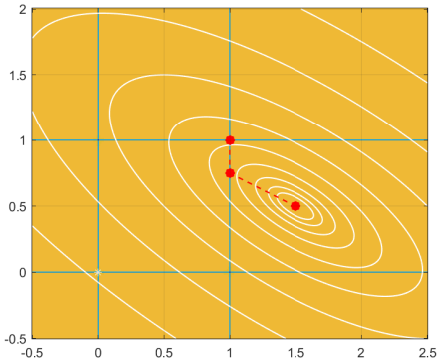

(d) $p = 0$.

Figure 3: Trajectory $\Gamma_{\lambda,p}$ (in red) followed by $\mathbf{u}^*_{\lambda,p}$ as a fonction of λ in the $u_1 - u_2$ plane.

non-regularized economic cost function $J_{\text{MPC}}(\mathbf{u},\mathbf{x})$ constrained by the time-varying model (6) does not present an analytical solution mainly because of the input matrix $\mathbf{B}_\xi\left(\mathbf{x}_z(k),\mathbf{q}_z^{Sol}(k),T_{\text{Ext}}(k)\right)$, which depends on the chosen control scenario. Thus, even if the non-convexity of the ℓ_ε-norm makes NP-Hard the regularized optimization problem, the complexity of the solving algorithm is not significantly increased with the regularization term. Although solvers such as "Interior Point OPTimizer" (IPOPT) (Wächter and Biegler, 2006) can efficiently find local solutions to nonlinear programming problems, these solutions are not particularly suited to our problem.

To solve this problem, we use a recently developed iterative algorithm (Gabsi et al., 2018b), the objective of which is to estimate the optimal control scenario with a controlled computation load. The idea is to keep at each time of prediction $k+j$ only a limited number of scenarios among all those that are possible. For this purpose, main component analysis is performed on a limited number of points judiciously chosen in the variables space $(T_{Op,z_1}(k+j), T_{Op,z_2}(k+j),\ldots,T_{Op,z_N}(k+j))$ in order to determine a suitable basis for the representation of all possible realizations of $T_{Op,z_i}(k+j)$ with $i = 1,\ldots,N$. By prioritizing the information, this makes it possible to replace the set of all these realizations by a smaller subset S_j whose cardinality is set a priori. This procedure is repeated N_p times in an iterative manner for j ranging from 1 to N_p. Of course, the larger the number $|S_j|$, the better the approximation of the optimal control scenario. This prioritization technique allows to consider not only a non-convex regularized criterion $J_{\lambda,\Omega}(\mathbf{u})$ (9) but also important values for the forecast time horizon N_P.

4.3 Application to the "Eco-Safe" Platform

The "Eco-Safe" platform consists of six zones and a corridor (Fig. 4). Each zone $z_i = \text{ⓘ}$ is equipped with several actuators and sensors to ensure a certain level of thermal comfort. The "research and development" room (R&D, zone z_1) and the "handling" room (zone z_5) are frequently occupied by students. They have a respective surface area of 51 m^2 and 34 m^2. Four other rooms, of 17 m^2 each, are used for the storage of different materials. The temperature of zones z_1 and z_5 can be controlled by two reversible air-to-air HPs that can generate hot and cold air. A CMV also allows air exchange between these two zones. A weather station integrating several sensors communicates with the platform and allows to know the different characteristics of the outside air.

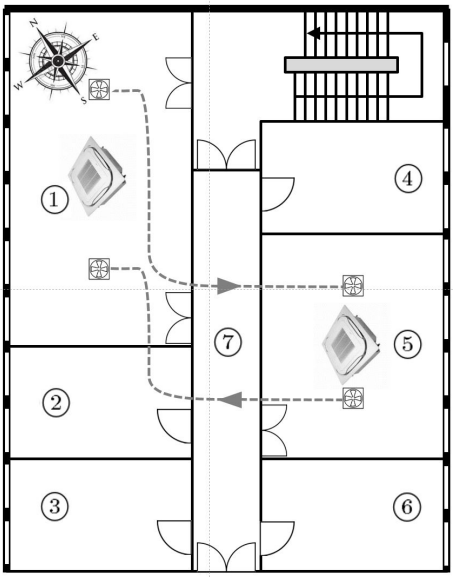

Figure 4: The "Eco-Safe" platform.

To illustrate the predictive control strategy presented above, we used a dynamic model of this platform established in (Gabsi et al., 2017). The latter integrates the thermal behaviour of all partitions/walls/windows in the zones as well as the different energy sources (solar radiation, occupants in the premises, HPs). It is possible to define 9 control scenarios:

- Scenario 0: no action on the system;
- Scenario 1: the CMV is switched on to circulate air from zone z_5 to zone z_1;
- Scenario 2: the CMV is switched on to circulate air from zone z_1 to zone z_5;
- Scenario 3: a HP is switched on in cooling mode (constant air flow, outlet temperature equal to 291 K) in zone z_1;
- Scenario 4: a HP is switched on in cooling mode in zone z_5;
- Scenario 5: both HPs are switched on in cooling mode in zones z_1 and z_5.
- Scenario 6: a HP is switched on in heating mode (constant air flow, outlet temperature equal to 313 K) in zone z_1;
- Scenario 7: a HP is switched on in heating mode in zone z_5;
- Scenario 8: both HPs are switched on in heating mode in zones z_1 and z_5.

The state-space model (6) associated with the platform is:

$$\begin{cases} \mathbf{x}_z(k+1) = \mathbf{A}_z\mathbf{x}_z(k) + \mathbf{F}_T T_{\text{Ext}}(k) + \mathbf{F}_q\mathbf{q}_z(k) + \\ \qquad\qquad \sum_{\xi=0}^{8} \mathbf{B}_\xi\left(\mathbf{x}_z(k), T_{\text{Ext}}(k)\right) u_\xi(k) \\ \mathbf{T}_z(k) = \mathbf{C}\mathbf{x}_z(k) \end{cases} \tag{18}$$

with:

- $\mathbf{T}_z(k) = \left[T_{z_1},\ T_{z_2},\ T_{z_4},\ T_{z_5},\ T_{z_7}\right]^T(k)$; no surface temperature is measured in zones z_i;
- $\mathbf{u}(k) = \left[u_\xi(k)\right]_{0\leq\xi\leq 8}$: the control vector formed of 0 and 1. It is defined as $u_\xi(k) = 1$ and $u_{\bar{\xi}}(k) = 0$ for all $\bar{\xi} \neq \xi$ when scenario u_ξ is implemented at time k;
- $\mathbf{q}_z(k) = \left[T_{\text{Ext}},\ Occ,\ Sol_{west},\ Sol_{East},\ T_{\text{HP}}\right]^T(k)$;
- $T_{\text{Ext}}(k)$: the outside temperature;
- $Occ(k)$: the number of occupants in zone z_1;
- $Sol_{west}(k)$ and $Sol_{East}(k)$: the energy provided by solar radiation for zones z_1, z_2, z_3 and z_4, z_5, z_6 resp.;
- $T_{\text{HP}}(k)$: the temperature of the air forced through the HPs, $T_{\text{HP}}(k) = 291$ K (cooling mode) or 313 K (heating mode).

Since the size of state vector $\mathbf{x}_z$ is very large (72-dimensional), the calculations required to develop a predictive control would become very complicated and time-consuming. The definition of a reduced order model is therefore necessary, based on a balanced state-space realization. In addition, as the purpose of this application example is mainly to demonstrate the interest of the regularisation terms, for the sake of simplicity and in accordance with Remark 1, the ambient air temperature in each zone z_i is considered into the economic cost function $J_{\text{MPC}}(\mathbf{u},\mathbf{x})$ (7), instead of the operative temperature:

$$J_{\text{MPC}}(\mathbf{u},\mathbf{x}) = \min_{\mathbf{u}} \sum_{j=1}^{N_P=12} \|\mathbf{T}_z(k+j) - 293\|^2_{\Psi_j} + \|\mathbf{u}(k+j)\|^2_{\epsilon_{\mathbf{u}_j}} \tag{19}$$

The reduced state vector is defined to correspond to the ambient air temperatures measured in each zone z_1, z_2, z_4, z_5 and z_7. Horizon N_p is chosen equal to 12 due to the sampling period which is 5mn. The forecast time horizon is therefore one hour depending on the platform's heating and cooling capacities. The weighting matrix Ψ_j is diagonal and time-variant. The ith term of diagonal $(\Psi_j)_{i,i}$ is zero if zone z_i is unoccupied at the time of prediction $k+j$. Otherwise, this term, which is chosen equal to $\psi_{z_i} > 0$, makes it possible to give more or less importance to the energy criterion (second part of (19)) compared to the

performance criterion (first part of (19)). For this illustration example, we will assume that only zone z_1 is occupied during standard working hours. The term $\|\Delta\mathbf{u}(k+j)\|^2_{\in'_{\Delta\mathbf{u}_j}}$ is not taken into account in the relationship (19) because the platform does not have automated closing/opening of tilt and turn windows or venetian blinds. As for the diagonal matrix $\in_{\mathbf{u}_j}$, it is defined according to the energy consumption of each of the scenarios (which is assumed to be constant no matter the day and time), namely:

$$\in_{\mathbf{u}_j} = \frac{1}{12} \times \text{diag}\left(\left[0\ 30\ 30\ 10^3\ 10^3\ 2000\ 10^3\ 10^3\ 2000\right]\right)$$

The regularisation term $\Omega(\mathbf{u})$ (17) takes the following form:

$$\Omega(\mathbf{u}) = \alpha_1 \|\mathbf{R_0 u} \odot (\mathbf{u}-\mathbf{1})\|^{\varepsilon}_{\varepsilon} + \alpha_2 \left(\left\|\mathbf{R_1 u}^{\text{HP}}_{z_1}\right\|^{\varepsilon}_{\varepsilon} + \left\|\mathbf{R_1 u}^{\text{HP}}_{z_5}\right\|^{\varepsilon}_{\varepsilon} \right) + \alpha_2 \left(\left\|\mathbf{R_1 u}^{\text{CMV}}_{z_1}\right\|^{\varepsilon}_{\varepsilon} + \left\|\mathbf{R_1 u}^{\text{CMV}}_{z_5}\right\|^{\varepsilon}_{\varepsilon} \right) \quad (20)$$

with a very large value for α_1. Regularization parameter λ (9) is taken as 0.5.

Fig. 7a to 7d represent over the period from 18 to 20 February 2019 the evolution of the ambient air temperatures $T_{z_1}(k)$ and $T_{z_5}(k)$ respectively associated with the control scenarios in Fig. 8a to 8d. The cumulative energy cost (in kWh) for each of these scenarios is shown in Fig. 9a to 9d respectively. The weather conditions present during this period at the platform location (Nancy, France) are reflected in Fig. 5a, 5b and 6a. The first two show the daily evolution of the solar energy entering the platform zones according to their orientation. The third figure shows the evolution of the outside temperature in K. Fig. 6b finally shows the number of occupants in zone z_1 (we will assume that each person emits 80W of internal heat gain). Fig. 8 represents as a function of time the value of the index ξ associated with the non-zero element of the vector $\mathbf{u}(k)$. A blue cross on a line ξ of these figures at time k therefore reflects the implementation of scenario ξ on the platform ($u_\xi(k) = 1$). For example, Fig. 8c shows that the non-zero element of $\mathbf{u}(k)$ over the entire first day is $u_0(k)$. This control scenario is associated with parameters $\psi_{z_1} = 1$ and $\alpha_2 = 3$. A simple analysis of these different figures shows:

- the influence of parameter ψ_{z_1}. The larger this parameter is compared to the terms of $\in_{\mathbf{u}_j}$, the greater the proportion of criterion $J_{\text{MPC}}(\mathbf{u},\mathbf{x})$ related to comfort performance increases at the expense of energy consumption. However, the lower this parameter is, the more important the energy aspect becomes compared to thermal comfort.
- the interest of the regularization term related to α_2. By comparing Fig. 8a and 8b with Fig. 8c and 8d respectively, it is clear that an increase in α_2 significantly reduces the number of switching (on/off) of VMCs and HPs. A direct consequence is the almost complete disappearance of the oscillations observed on $T_{z_1}(k)$ and $T_{z_5}(k)$ (Fig. 7d vs. Fig. 7b).
- the interest of the regularization term in α_1 which allows to privilege discontinuous optimal values for $\mathbf{u}$ during the optimization of the regularized criterion. For this illustration example, only values 0 and 1 are allowed for all elements of $\mathbf{u}$.

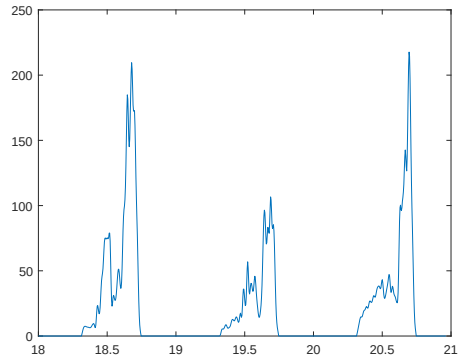

(a) $Sol_{West}(k)$; $z_i = z_1, z_2, z_3$.

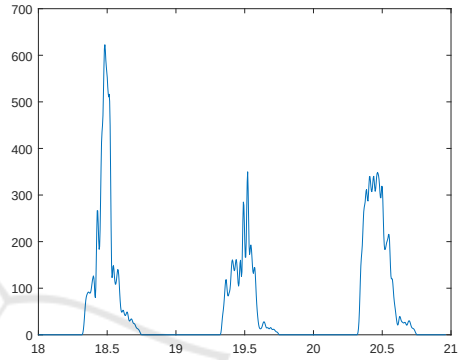

(b) $Sol_{East}(k)$; $z_i = z_4, z_5, z_6$.

Figure 5: Energy (W/m^2) provided by solar radiation for zones z_i.

5 CONCLUSION

This paper aims to optimize the energy efficiency of multizone buildings by implementing a regularized economic model predictive controller (REMPC). More precisely, the objective is to maintain thermal comfort in occupied zones while minimizing energy consumption.

To achieve this long-term overall objective, an economic cost function was first defined and control specifications were added via a regularization crite-

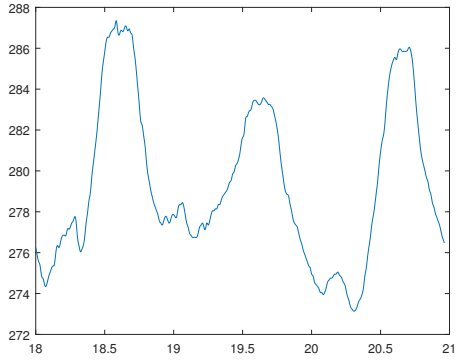

(a) Outside temperature T_{Ext} (K).

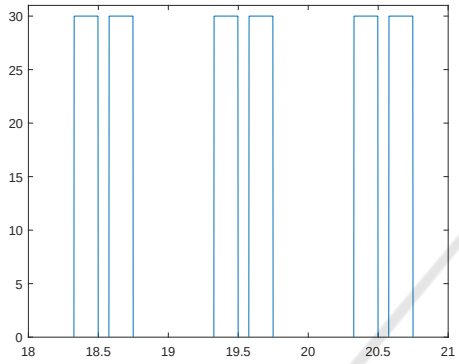

(b) Number of occupants Occ.

Figure 6: Disturbances $\mathbf{q}(k)$ (in addition to solar radiation).

rion. The first regularized term concerns the limitation of the frequency of on/off cycles for particular actuators such as HPs or VMCs. Indeed, the very frequent starting and stopping of this type of equipment makes inefficient their energy operating mode and can especially lead to severe damages. Other criteria related to the number of actuators used at a given time or to the discrete nature of certain control variables were also taken into account in the regularized criterion. An analysis showed the importance of choosing an appropriate ℓ_p-norm to define these regularization terms. It has been shown that a ℓ_ε-norm is to be preferred.

This control strategy was tested on a platform simulator (Gabsi et al., 2017) located in the CRAN laboratory (Nancy/France) and gave very encouraging results for on-site implementation.

ACKNOWLEDGEMENTS

This work has financial support from the Contrat de Plan Etat-Région (CPER) 2015-2020, project "Matériaux, Energie, Procédés".

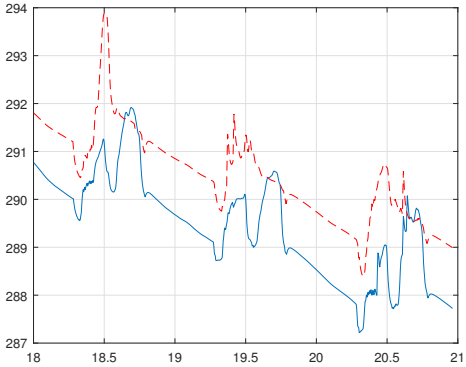

(a) $\psi_{z_1} = 1$, $\alpha_2 = 0$.

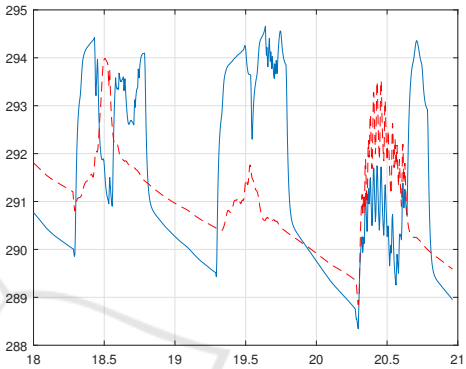

(b) $\psi_{z_1} = 20$, $\alpha_2 = 0$.

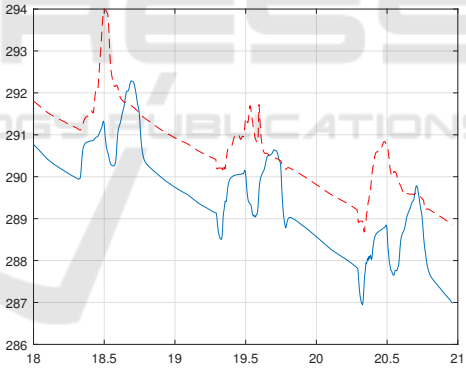

(c) $\psi_{z_1} = 1$, $\alpha_2 = 3$.

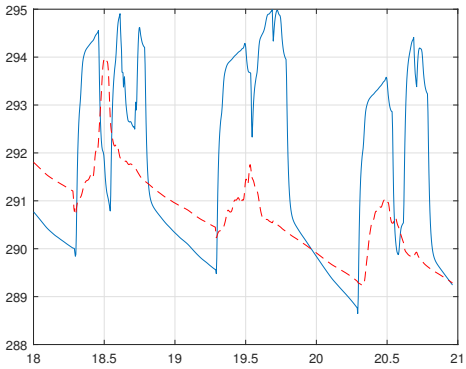

(d) $\psi_{z_1} = 20$, $\alpha_2 = 10$.

Figure 7: Ambient air temperatures T_{z_1} (K, in solid blue line) and T_{z_5} (K, in red dashed line).

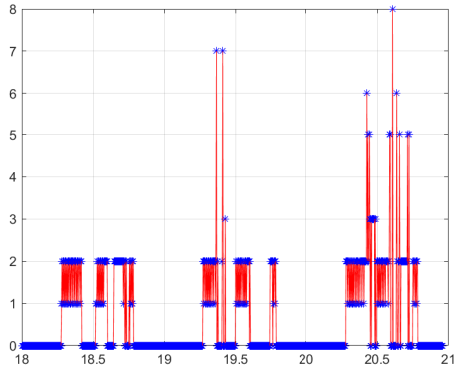

(a) $\psi_{z_1} = 1$, $\alpha_2 = 0$.

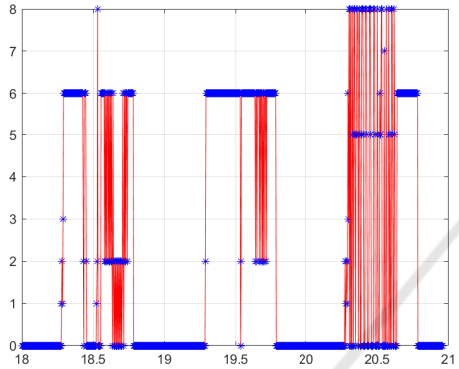

(b) $\psi_{z_1} = 20$, $\alpha_2 = 0$.

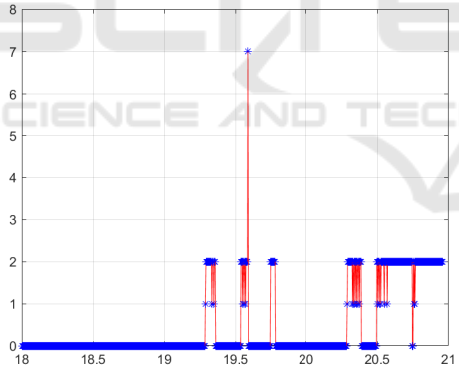

(c) $\psi_{z_1} = 1$, $\alpha_2 = 3$.

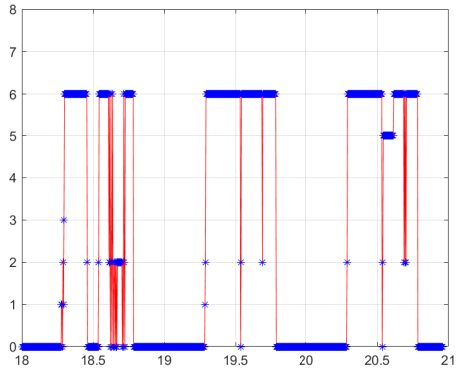

(d) $\psi_{z_1} = 20$, $\alpha_2 = 10$.

Figure 8: Control scenarios.

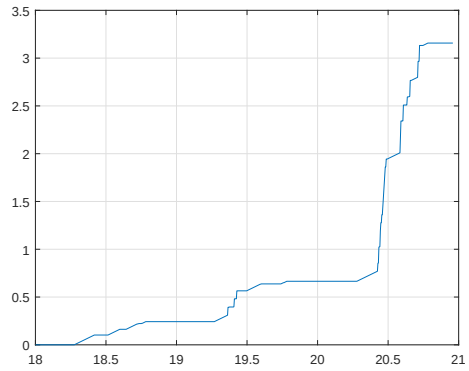

(a) $\psi_{z_1} = 1$, $\alpha_2 = 0$.

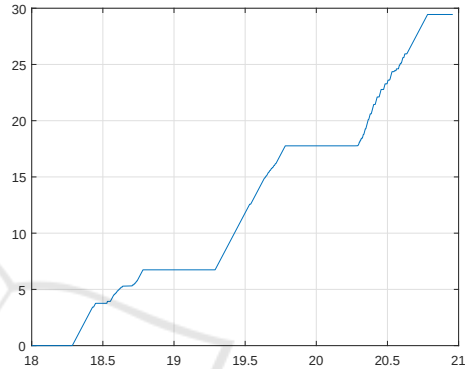

(b) $\psi_{z_1} = 20$, $\alpha_2 = 0$.

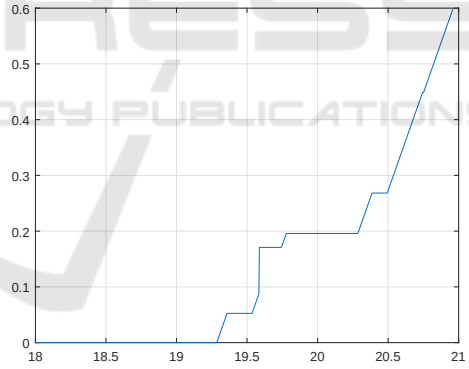

(c) $\psi_{z_1} = 1$, $\alpha_2 = 3$.

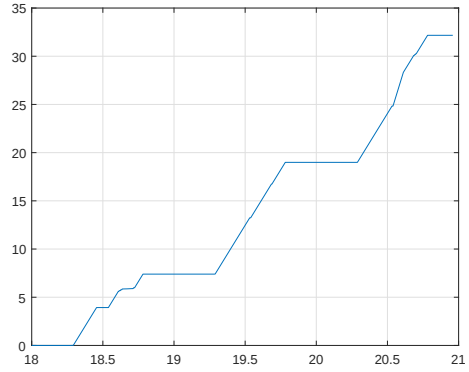

(d) $\psi_{z_1} = 20$, $\alpha_2 = 10$.

Figure 9: Cumulative energy cost (kWh).

REFERENCES

Aguilera, R. P., Delgado, R., Dolz, D., and Agüero, J. C. (2014). Quadratic MPC with l_0-input constraint. *IFAC Proceedings Volumes*, 47(3):10888 – 10893.

Aguilera, R. P., Urrutia, G., Delgado, R. A., Dolz, D., and Agüero, J. C. (2017). Quadratic model predictive control including input cardinality constraints. *IEEE Transactions on Automatic Control*, 62(6):3068–3075.

Amy, T., Kong, H., Auger, D., Offer, G., and Longo, S. (2016). Regularized MPC for power management of hybrid energy storage systems with applications in electric vehicles. *IFAC-PapersOnLine*, 49(11):265 – 270.

Challapalli, N., Nagahara, M., and Vidyasagar, M. (2017). Continuous hands-off control by clot norm minimization. *IFAC-PapersOnLine*, 50(1):14454 – 14459. 20th IFAC World Congress.

Cho, K.-j. and Cho, D.-w. (2018). Solar heat gain coefficient analysis of a slim-type double skin window system: Using an experimental and a simulation method. *Energies*, 11(1).

Cojocaru, E. G., Bravo, J. M., Vasallo, M. J., and Marín, D. (2020). A binary-regularization-based model predictive control applied to generation scheduling in concentrating solar power plants. *Optimal Control Applications and Methods*, 41(1):215–238.

Ellis, M., Durand, H., and Christofides, P. D. (2014). A tutorial review of economic model predictive control methods. *Journal of Process Control*, 24(8):1156 – 1178.

Engl, H. W., Hanke, M., and Neubauer, A. (1996). *Regularization of inverse problems*, volume 375. Springer Science & Business Media.

Gabsi, F., Hamelin, F., Pannequin, R., and Chaabane, M. (2017). Energy efficiency of a multizone office building: MPC-based control and simscape modelling. In *2017 International Conference on Smart Cities and Green ICT Systems (SMARTGREENS)*, pages 227–234, Porto, Portugal. INSTICC.

Gabsi, F., Hamelin, F., and Sauer, N. (2018a). Building hygrothermal modeling by nodal method. In *2018 IEEE PES Innovative Smart Grid Technologies Conference Asia (ISGT)*, Singapore.

Gabsi, F., Hamelin, F., and Sauer, N. (2018b). Hygrothermal modelling and MPC-based control for energy and comfort management in buildings. In *2018 International Conference on Smart Grid and Clean Energy Technologies (ICSGCE)*, Kajang, Malaysia.

Gallieri, M. and Maciejowski, J. M. (2012). l_{asso} MPC: Smart regulation of over-actuated systems. In *2012 American Control Conference (ACC)*, pages 1217–1222.

Gallieri, M. and Maciejowski, J. M. (2015). Model predictive control with prioritised actuators. In *2015 European Control Conference (ECC)*, pages 533–538.

Godina, R., Rodrigues, E. M. G., Pouresmaeil, E., Matias, J. C. O., and Catalão, J. P. S. (2018). Model predictive control home energy management and optimization strategy with demand response. *Applied Sciences*, 8(3).

Hastie, T., Tibshirani, R., and Friedman, J. (2009). *The elements of statistical learning: data mining, inference and prediction*. Springer, 2 edition.

McCartney, K. J. and Nicol, J. F. (2002). Developing an adaptive control algorithm for europe. *Energy and Buildings*, 34(6):623 – 635. Special Issue on Thermal Comfort Standards.

Nagahara, M., Quevedo, D. E., and Østergaard, J. (2014). Sparse packetized predictive control for networked control over erasure channels. *IEEE Transactions on Automatic Control*, 59(7):1899–1905.

Pakazad, S. K., Ohlsson, H., and Ljung, L. (2013). Sparse control using sum-of-norms regularized model predictive control. In *52nd IEEE Conference on Decision and Control*, pages 5758–5763.

Rao, C. V. (2018). Sparsity of linear discrete-time optimal control problems with l_1 objectives. *IEEE Transactions on Automatic Control*, 63(2):513–517.

Rawlings, J. B., Patel, N. R., Risbeck, M. J., Maravelias, C. T., Wenzel, M. J., and Turney, R. D. (2018). Economic MPC and real-time decision making with application to large-scale HVAC energy systems. *Computers & Chemical Engineering*, 114:89 – 98.

Rockett, P. and Hathway, E. A. (2017). Model-predictive control for non-domestic buildings: a critical review and prospects. *Building Research & Information*, 45(5):556–571.

Serale, G., Fiorentini, M., Capozzoli, A., Bernardini, D., and Bemporad, A. (2018). Model predictive control (MPC) for enhancing building and HVAC system energy efficiency: Problem formulation, applications and opportunities. *Energies*, 11(3).

Tibshirani, R. (1994). Regression shrinkage and selection via the lasso. *Journal of the Royal Statistical Society, Series B*, 58:267–288.

Tibshirani, R., Saunders, M., Rosset, S., Zhu, J., and Knight, K. (2005). Sparsity and smoothness via the fused lasso. *Journal of the Royal Statistical Society. Series B (Statistical Methodology)*, 67(1):91–108.

Wächter, A. and Biegler, L. (2006). On the implementation of an interior-point filter line-search algorithm for large-scale nonlinear programming. *Mathematical programming*, 106:25–57.

Zhuang, J., Chen, Y., and Chen, X. (2018). A new simplified modeling method for model predictive control in a medium-sized commercial building: A case study. *Building and Environment*, 127:1 – 12.

Zong, Y., Böning, G. M., Santos, R. M., You, S., Hu, J., and Han, X. (2017). Challenges of implementing economic model predictive control strategy for buildings interacting with smart energy systems. *Applied Thermal Engineering*, 114:1476 – 1486.